Biosensors and Bioelectronics 41 (2013) 225–231

Contents lists available at SciVerse ScienceDirect

Biosensors and Bioelectronics

journal homepage: www.elsevier.com/locate/bios

Highly sensitive and selective dopamine biosensor based on 3,4,9,10-perylene tetracarboxylic acid functionalized graphene sheets/multi-wall carbon nanotubes/ionic liquid composite film modified electrode

Xiuli Niu, Wu Yang*, Hao Guo, Jie Ren, Jinzhang Gao

College of Chemistry and Chemical Engineering, Key Lab of Bioelectrochemistry and Environmental Analysis of Gansu Province, Northwest Normal University, Lanzhou 730070, PR China

ARTICLE INFO

Article history:
Received 6 May 2012
Received in revised form
8 August 2012
Accepted 9 August 2012
Available online 23 August 2012

Keywords:
Graphene
Multi-wall carbon nanotubes
Ionic liquid
3,4,9,10-perylene tetracarboxylic acid
Dopamine
Modified electrode

ABSTRACT

A sensitive and selective electrochemical sensor for determination of dopamine (DA) was fabricated based on 3,4,9,10-perylene tetracarboxylic acid functionalized graphene sheets, multi-wall carbon nanotubes and ionic liquid modified glass carbon electrode and the properties of modified electrode were characterized by scanning electron microscopy, transmission electron microscope and electrochemical impedance spectroscopy. The modified electrode showed excellent electrocatalytic activity toward the oxidation of DA. Meanwhile, a possible reaction mechanism related to the oxidation of DA was proposed. The differential pulse voltammetry was used for the determination of DA in the presence of 500 μM ascorbic acid and 330 μM uric acid under the optimum conditions and a good linear relationship between peak current and the concentration of DA was obtained in the concentration range from 0.03 μM to 3.82 mM with a detection limit of 1.2×10^{-9} M (S/N=3). Moreover, the proposed method was successfully applied to determine DA in real sample and satisfactory results were obtained. The results showed that the modified electrode exhibits an excellent catalytic activity, good sensitivity, reproducibility and long-term stability.

1. Introduction

Sensitive, selective, rapid, and cost-effective analysis of biomolecules is important in clinical diagnostics and treatment. Carbon nanostructures, such as carbon nanotubes, carbon nanodots, and carbon nanofibers have been used for this purpose (Liu et al., 2008a; Chen et al., 2007; Cao et al., 2007; Fu et al., 2007; Hao et al., 2007). Recently, graphene-based nanomaterials have attracted great attention for both fundamental science and applied research. Graphene is a two-dimensional sheet of carbon atoms bonded by sp^2 hybrid orbitals. This structural characteristic is the reasons for the extraordinary properties of graphene, which include a very large surface area, high electrical conductivity, exceptional thermal and mechanical properties (Geim and Novoselov, 2007). Because of their novel properties, graphene sheets (GS) have received considerable interest for potential applications in many fields, such as nanocomposites, field-effect transistors, biosensors, and so on. It is noted that GS, which have a high specific surface area, tend to form irreversible agglomerates or even restack to form graphite through strong π–π stacking and van der Waals interaction (Li et al., 2008). Hence the prevention of aggregation is a key challenge in the synthesis and processing of bulk-quantity GS. Recently, it has been found that the functionalization is an efficient method to improve their dispersibility and solubility in aqueous solvent (Zhang et al., 2011; Liu et al., 2010; Li et al., 2009; Hong et al., 2010). It is well known that carbon nanotubes(CNTs) are suitable materials for electrode modification because of the high accessible surface area, low electrical resistance, extremely high mechanical strength and stiffness, outstanding charge-transfer characteristics and high chemical stability (Fang et al., 2009; Guldi et al., 2005; Dai et al., 2006; Rodney et al., 2002). The application of CNTs in the fields of electroanalysis and electrochemical biosensors had been reviewed. Generally, CNTs can enhance the detection sensitivity and improve reversibility as it can promote electron transfer.

On the other hand, ionic liquid (IL) have also received great attention in the last few years due to their excellent properties such as high ionic conductivity, good chemical and thermal stability, negligible vapor pressure, wide electrochemical windows and well biocompatibility. IL can be used as not only the supporting electrolyte but also the modifier for the chemically modified electrodes. The reviews about the application of IL in the

* Corresponding author. Tel.: +86 931 7971216.
E-mail address: xbsfda123@126.com (W. Yang).

0956-5663/$ - see front matter © 2012 Elsevier B.V. All rights reserved.
http://dx.doi.org/10.1016/j.bios.2012.08.025

fields of analytical chemistry or electrochemistry had been reported (Pandey, 2006; Sun et al., 2007). Several groups had used different kinds of IL in electrode modification for the design of new electrochemical sensors or as novel electrocatalytic materials. The studies demonstrated that the presence of IL not only acted as a suitable charge-transfer bridge to facilitate the electrode transfer rate but also exhibited excellent electrocatalytic ability and good anti-fouling ability (Sun et al., 2009a,b; Shul et al., 2006; Choi et al., 2009).

Dopamine (DA) is an important neurotransmitter in the mammalian central nervous system. Low levels of DA may cause neurological disorders such as schizophrenia and Parkinson's disease (Liu et al., 2005; Mo and Ogorevc, 2001). The accurate and rapid determination of DA concentration in body fluid is a significant issue to conveniently trace and diagnose the diseases. Ascorbic acid (AA) is well known for its antioxidant property and usually coexists with DA in biological samples, which concentration is several orders of magnitude higher than that of DA, and have a similar oxidation potential (Yen et al., 2002; Ali et al., 2007; Tang et al., 2008). Therefore, it is of importance to develop a rapid, simple, sensitive sensor for the detection of DA without interference by AA. Recently, different kinds of DA sensors have been fabricated based on chemical modified electrodes, such as polymer electrodes, self-assembled monolayer and carbon nanomaterial film electrodes (Codognoto et al., 2007; Lakshmi et al., 2009; Rodriguez et al., 2008; Kalimuthu and Abraham, 2010; Liu et al., 2008b; Zhu et al., 2009; Kim et al., 2010; Thiagarajan et al., 2009). Graphene and CNTs have widely been used as ideal electrode modified nanomaterials because they can provide more active sites and are easier to fabricate. Several groups had used functionalized graphene, CNTs or negatively charged polymer films to modify electrodes to determination positively charged DA and to eliminate the interference of AA (Hou et al., 2010; Deng et al., 2009; Zhao et al., 2005; Wang et al., 2009; Balamurugan and Chen, 2007). Although the electrochemical responses have been continuously improved, the development of more reliable and efficient sensors for sensitive analysis of DA still remains very challenging. Therefore, the choice of material is essential and important to construct sensors with excellent performances.

In this paper, 3,4,9,10-perylene tetracarboxylic acid functionalized graphene sheets (PTCA-GS) were prepared by a simple synthetic method. The modification of PTCA onto graphene sheets can not only separate the graphene sheets and maintain inherent electronic structure of graphene sheets but also provide a negatively-charged –COOH, which made the resulting PTCA-GS composites disperse well in solvents and provide more active sites. Meanwhile, by combining the advantages of PTCA-GS, MCNT and IL, a novel and more sensitive dopamine electrochemical sensor was fabricated with PTCA-GS/MCNT/IL modified electrodes. Because of synergetic effects of conductive functionalized graphene, MCNT and biocompatible IL, the direct electron transfer between DA and electrode surface can be efficiently achieved. Most importantly, such modified electrode shows good electrocatalytic performance to DA with high sensitivity and good stability. The sensitivity of the sensor along with its improved selectivity might allow for its potential use in the investigation and diagnosis of dopamine-related disease.

2. Materials and methods

2.1. Reagents

Natural graphite powder ($<20\ \mu m$) was purchased from Tianjin Guangfu Research Institute (Tianjin, china). Multi-walled carbon nanotubes (purity $>95\%$) was purchased from Shenzhen Nanotech Port Company (Shenzhen, China). [BMIM][BF_4] was purchased from Lanzhou Institute of Chemical Physics (Lanzhou, China). 3,4,9,10-perylenetetracarboxylic dianhydride (PTCDA, 97%), dopamine, ascorbic acid and uric acid were ordered from Sigma-Aldrich (USA). The 3,4,9,10-perylene tetracarboxylic acid (PTCA) solution was made by hydrolyzing 3,4,9,10-perylenete-tracarboxylic dianhydride (PTCDA) in an appropriate amount of 1.0 M sodium hydroxide. Phosphate buffer solution (PBS) was prepared by mixing the stock solution of 0.1 M NaH_2PO_4 and 0.1 M Na_2HPO_4 and adjusting the pH with 0.1 M H_3PO_4 or 0.1 M NaOH. Unless otherwise stated, other reagents were of analytical grade and were used as received. All aqueous solutions were prepared with double distilled water.

2.2. Apparatus

Electrochemical experiments were performed on a CHI-832 electrochemical workstation (CH Instruments, Shanghai Chenhua Instrument Corporation, China). A three-electrode cell was employed, consisting of a glassy carbon electrode (GCE) or a modified GCE as a working electrode, saturated calomel electrode (SCE) and platinum sheet respectively as the reference and auxiliary electrode. All potentials are referred to the SCE. The electrochemical impedance spectroscopy measurements were performed on a VMP2 multichannel potentiostats. Scanning electron microscopy (SEM) images were determined with a JSM-6701 F field emission scanning electron microscope (Japanese Electron Optics Company). Transmission electron microscope (TEM) images were obtained with a JEM 1200EX transmission electron microscope opened at an accelerating voltage of 80.0 KV (Japanese Electron Optics Company).

2.3. Synthesis of graphene and PTCA-functionalized graphene sheets

Synthesis of graphene: graphite oxide (GO) was synthesized from graphite powder by a modified Hummers method. GS were prepared by the chemical reduction of GO with hydrazine. Typically, GO (100 mg) was dispersed in 100 mL of deionized water and the dispersion was sonicated using a KQ-250DE ultrasonic bath cleaner until it became clear with no visible particulate matter. Hydrazine monohydrate (1 mL) was then added to the dispersion and the mixture was heated in an oil bath at 100 °C for 24 h. After the completion of the reaction, the reduced graphite oxide was collected by filtration, followed by washing with deionized water several times to remove excess hydrazine. The final product was dried in a vacuum oven at 80 °C for 24 h.

Synthesis of PTCA-GS: PTCA-GS was prepared by a simple synthetic method. Typically, PTCA (7.4 mg) and GO (30.0 mg) were dispersed in 25.0 mL water and then stirred at 40 °C for 24 h. Subsequently, hydrazine solution (0.5 mL) and ammonia solution (0.5 mL) were added to the mixture and the reaction mixture was held at 90 °C for 50 min under vigorous agitation. Finally, the precipitation was filtered, washed with deionized water for five times, and dried in a vacuum oven at 25°C.

2.4. Fabrication of PTCA-GS/MCNT/IL, MCNT/IL and PTCA-GS/IL modified electrodes

Before the modification, GCE (3 mm) were carefully polished to a mirror with 1.0 μm, 0.3 μm and 0.05 μm alumina slurry in sequence, rinsed thoroughly with doubly distilled water between each polishing step, finally sonicated in 1:1 HNO_3, 1:1 ethanol, and doubly distilled water, and dried under a nitrogen stream. And then the electrode was immersed in 1.0 M H_2SO_4 and treated by cyclic voltammetric scanning in the potential range of -1.0 to $+1.0$ V (vs. saturated calomel electrode, SCE) until a stable CV profile was obtained. For the preparation of PTCA-GS/MCNT/IL/GCE, MCNT/IL/GCE and PTCA-GS/IL/GCE, 10 mL of 0.1 mg mL^{-1} PTCA-GS/MCNT was first mixed with 50 μL of IL and sonicated for 2 h to form a homogenous mixture. Then, 5 μL of the mixture was dropped on the pretreated GCE with a microsyringe and dried for 24 h in air before

use. MCNT/IL/GCE, PTCA-GS/IL/GCE were also fabricated for comparison using similar process just using MCNT and PTCA-graphene sheets instead of PTCA-GS/MCNT, respectively.

3. Results and discussion

3.1. Characterization of GS, PTCA-GS and PTCA-GS/MCNT/IL composite film

The morphology of GS, PTCA-GS and PTCA-GS/MCNT/IL composite film was characterized using SEM and TEM. Fig.1A and C shows the surface morphology of GS and PTCA-GS, respectively. It can be seen that the unfunctionalized graphene sheets tended to restack with one another, remarkably reducing the useful surface area. In addition, the lateral size of the nanosheets ranged from several hundred nanometers to several micrometers in length. As shown in Fig.1B, graphene sheets exhibited as ultrathin transparent nanosheets and the transparent sheets were flake-like with wrinkles. In contrast, the SEM (Fig. 1C) and TEM (Fig. 1D) images of PTCA-GS show a more uniform surface topography. Moreover, ultrathin transparent nanosheet of PTCA-GS show three-dimensional network-like structure. The intergraphene gaps are clearly less than 1 nm, and this porous structure could

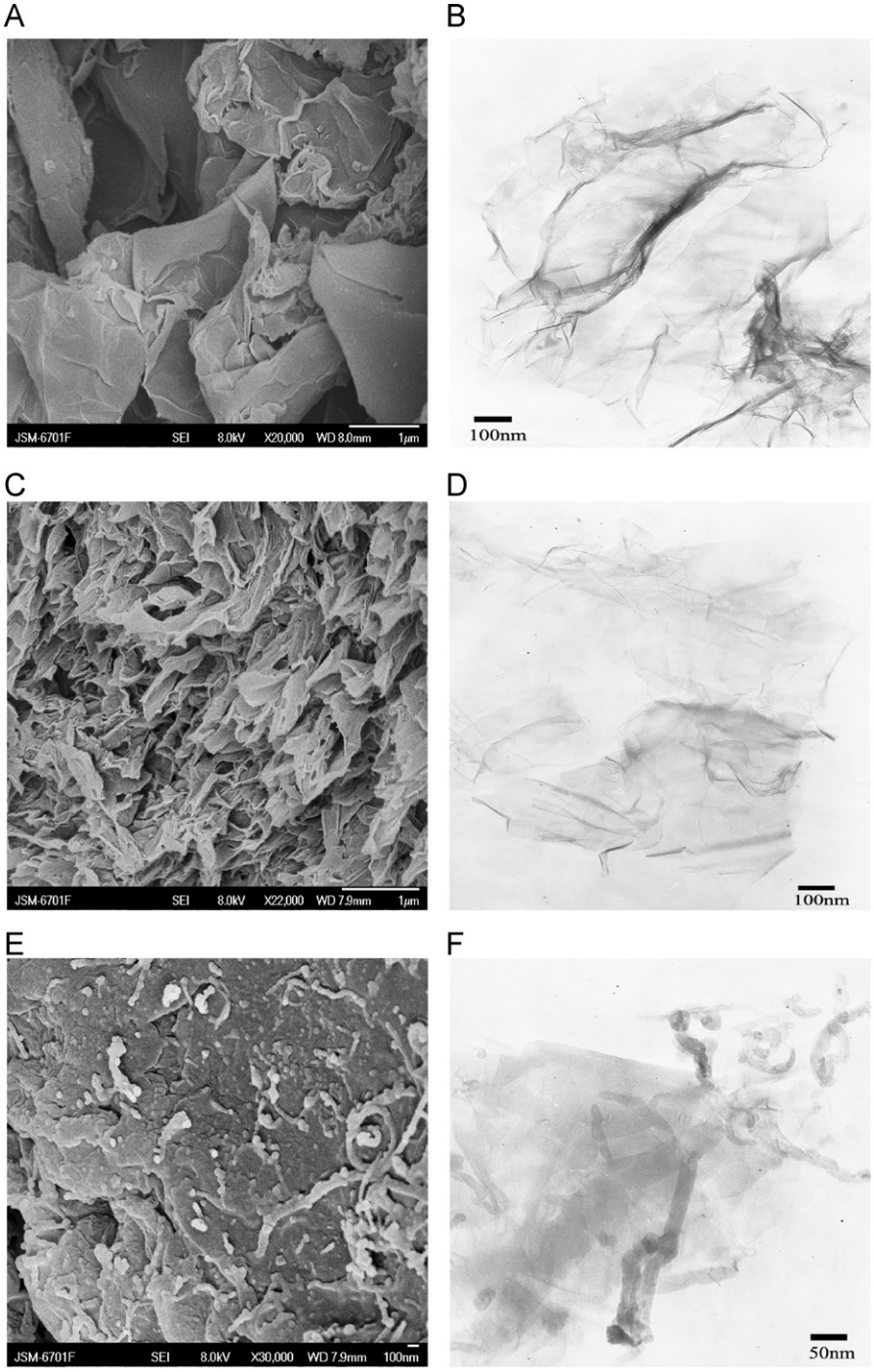

Fig. 1. (A) SEM image of graphene sheets, (B) TEM image of graphene sheets, (C) SEM image of PTCA-functionalized graphene sheets, (D) TEM image of PTCA-functionalized graphene sheets, (E) SEM image of PTCA-GS/MCNT/IL composite film and (F) TEM image of PTCA-GS/MCNT/IL composite film.

significantly increase the effective electrode surface and facilitate the diffusion of the analytes into the film. PTCA not only behave as a modifier of graphene, altering their surface property and preventing their possible agglomeration, but also act as a linkage between graphene and the analytes. The SEM and TEM images of the PTCA-GS/MCNT/IL composite film are shown in Fig.1E and F. It can be seen that interwoven PCTA-GS and MCNT formed a layer of well distributed and steady thin film under the high conductivity of IL. Moreover, a well-packed, highly ordered structure film of PTCA-GS/MCNT/IL was formed during the drying process of the PTCA-GS/MCNT/IL suspension mixture. The nanosized composite film contained a large amount of open graphitic edge planes, which may facilitate the improvement of the electrochemical behaviors. Once deposited on the GCE surface, PTCA-GS, MCNT and IL tended to form a uniform film on the GCE surface. The uniform surface, along with the high conductivity of PTCA-GS, MCNT and IL, provided a favorable environment for electrochemical tests of biomolecules, such as DA.

3.2. Electrochemical characteristics of the modified electrodes

Electrochemical impedance spectroscopy (EIS) was employed to monitor the modifying process of electrode. Fig. 2 shows the typical EIS results of different modified electrodes in 10.0 mM $[Fe(CN)_6]^{3-/4-}$ solution. By fitting the data using an appropriate equivalent circuit, the charge transfer resistance (R_{ct}) of the bare GCE was obtained as 2937 Ω (curve a). After modification with IL, the R_{ct} decreased dramatically to 1786 Ω (curve b), indicating the presence of high ionic conductive IL could greatly enhance the conductivity of the electrode and facilitated the electron transfer between solution and electrode interface. After IL-modified GCE was further modified with MCNT (curve c) and PTCA-GS (curve d) respectively, the EIS exhibited very low interfacial R_{ct} and the R_{ct} values decreased significantly to 556.3 Ω and 474.9 Ω, which demonstrated that the PTCA-GS/IL/GCE and MCNT/IL/GCE could effectively improve the conductivity of the electrode and have higher electrochemical activity than bare GCE and IL/GCE. While on the PTCA-GS/MCNT/IL/GCE, a nearly straight line was obtained with the R_{ct} value close to zero (curve e), indicating the higher conductivity. Though the surfaces of PTCA-GS and MCNT have a quantity of negative change, it cannot totally hinder the diffusion of high concentration (10 mM) of $[Fe(CN)_6]^{3-/4-}$ towards the electrode surface. Moreover, these results also indicated that the PTCA-GS, MCNT and IL were successfully modified on the surface of GCE and promoted the electrode transfer.

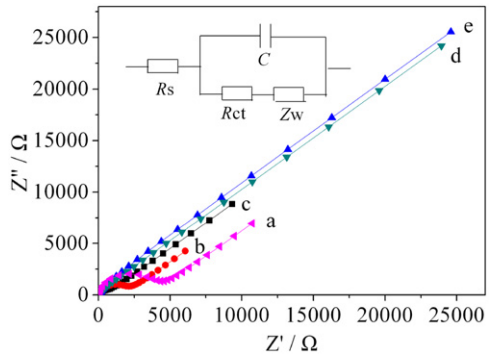

Fig. 2. Electrochemical impedance spectroscopy for (a) bare GCE, (b) IL/GCE, (c) MCNT/IL/GCE, (d) PTCA-GS/IL/GCE, (e) PTCA-GS/MCNT/IL/GCE in the solution of 10.0 mM $[Fe(CN)_6]^{3-/4-}$ and 0.1 M KCl with the frequencies swept from 10^5 to 0.1 Hz. Inset is the Randles circuit model for the modified electrodes. R_s: solution resistance; R_{ct}: charge-transfer resistance; C: double-layer capacitance; Z_w: Warbury resistance.

3.3. Electrochemical behavior of DA

The electrochemical behaviors of DA at the bare and modified electrodes were investigated by cyclic voltammogram (CV) in 0.1 M PBS (pH 5.0) containing 110 μM DA. As shown in Fig. 3A, a pair of small and unsymmetrical redox peaks appeared on the bare GCE (curve a) with an anodic peak (E_{pa}) and a cathodic peak (E_{pc}) respectively at 0.397 and 0.196 V and peak-to-peak separation (ΔE_p) was calculated as 201 mV, which indicated that the direct electron transfer of DA on bare GCE was very slow and irreversible. However, on the PTCA-GS/MCNT/IL/ GCE (curve d) appeared a pair of well-defined redox peaks with E_{pa} and E_{pc} respectively at 0.229 and 0.288 V and ΔE_p was calculated as 59 mV, which indicated that a quasi-reversible electrochemical reaction of DA took place and the redox reaction was very fast. The peak current increased for about 2.4-fold larger than that on the bare GCE. The higher redox currents and more negative

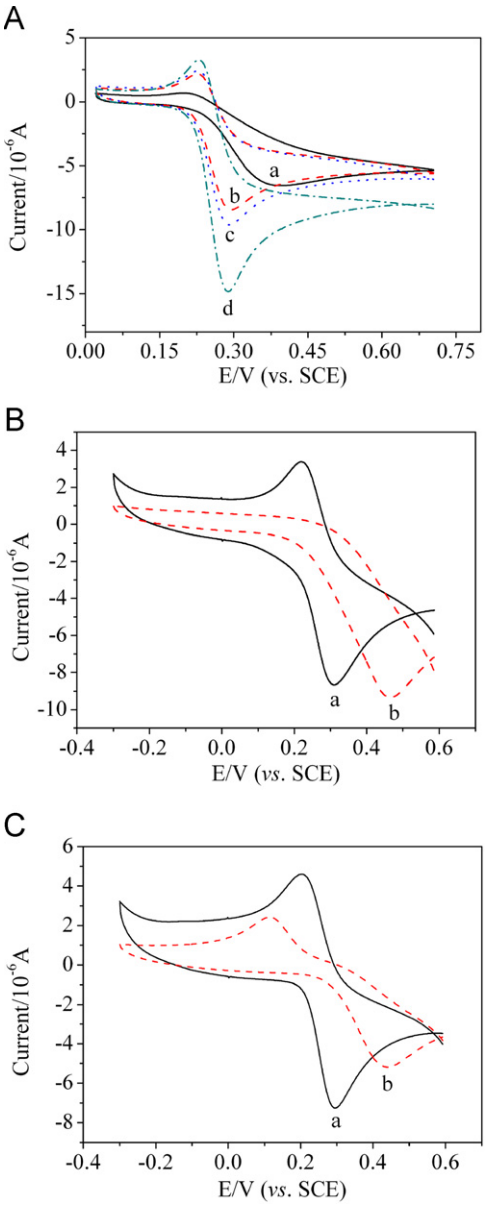

Fig. 3. (A) The cyclic voltammograms of 110 μM DA at the bare GCE (a), MCNT/IL/GCE (b), PTCA-GS/IL/GCE (c), PTCA-GS/MCNT/IL/GCE (d); Typical cyclic voltammograms of 50 μM DA in the presence of 125 μM AA (B) and in the absence of AA (C) at the bare GCE (dotted line) and PTCA-GS/MCNT/IL modified electrode (full line) in 0.1 M PBS (pH 5.0). Scan rate: 60 mV s^{-1}.

oxidation potential suggested that PTCA-GS/MCNT/IL/GCE had a good electrocatalytic ability to the electrochemical reaction of DA. The MCNT/IL/GCE (curve b) and PTCA-GS/IL/GCE (curve c) showed a quite low anodic peak potential at 0.223 V, 0.226 V respectively. The peak currents increased about 1.33-fold, 1.4-fold larger than that on the bare GCE. The decrease of overpotential and the increase of redox peak currents demonstrated that the MCNT/IL and PTCA-GS/IL modified electrode could facilitate the oxidation of DA greatly. Compared to bare GCE, MCNT/IL and PTCA-GS/IL modified electrode, the PTCA-GS/MCNT/IL modified electrode possessed high conductivity, larger surface areas, uniform structure, efficient catalytic activity and biocompatibility. The synergistic effect of PTCA-GS, MCNT and IL in the composite film can facilitate the electron transfer rate and increase the oxidation signals significantly. The presence of IL not only promoted the electron transfer but also exhibited excellent electrocatalytic ability and good anti-fouling ability.

Fig. 3B and C shows cyclic voltammograms for the oxidation of DA in the presence and absence of AA at the bare and modified electrode. 50 μM DA and 125 μM AA in 0.1 M PBS (pH 5.0) showed an irreversible broad oxidation peak at 0.465 V at the bare GCE (Fig. 3B(b)). But at the PTCA-GS/MCNT/IL/GCE appeared well-shaped redox peaks (Fig. 3B(a)) with a remarkable increase in redox currents and negative shift of oxidation peak potential(0.309 V). Due to the strong electrostatic repulsion between AA and PTCA-GS/MCNT/IL composite film, the electrochemical oxidation of AA was inhibited seriously. Thus, no currents response could be seen. In absence of AA, similar results were observed (Fig. 3C). The current responses of DA in the absence and presence of AA were approximately equal, which indicated that oxidation of DA took place on the modified electrode without any interference from AA. The extraordinarily electrocatalytic activity of the modified electrode may be attributed to the high specific surface area and excellent electron transfer ability of the PTCA-GS/MCNT/IL film. Because PTCA and acid-pretreated MCNT introduce more negatively charged (–COOH, –OH) without further destroying the conjugation of graphene and MCNT. The PTCA-GS/MCNT/IL composite film can concentrate the DA from solution due to electrostatic attraction of the positively charged DA and the negatively charged group. At the same time, the PTCA-GS/MCNT/IL composite film can block the diffusion of AA by the electrostatic repulsion of the negatively charged AA and the negatively charged group. Therefore, the PTCA-GS/MCNT/IL modified electrode eliminated AA interference and increased the selectivity and sensitivity. The determination of DA could be achieved even in the presence of high concentration of AA.

3.4. Optimization of condition

3.4.1. Effect of accumulation potential and time

Accumulation can improve the amount of adsorption of DA at the electrode and enhance its oxidation signal, which resulted in an improvement of the sensitivity. Fig. S1A shows that the peak current of DA rapidly increased with increasing accumulation time and then decreased with the further increase, and the maximum peak currents was obtained at 60 s. The peak current of DA at 60 s was about 3-times larger than that without accumulation. Therefore, the accumulation time of 60 s was chosen as the optimum value for further experiments. Fig. S1B shows the effect of accumulation potential on the CV peak current of 100 μM DA after 60 s accumulation. The peak current slightly increased and then decreased as the potentials shifted negatively from 0.6 to −0.3 V. The maximal peak current was observed at 0.2 V. Therefore, 0.2 V was applied as the optimal accumulation potential.

3.4.2. Effect of the solution pH

Proton is always involved in the electrochemical reaction of organic compound and exerts significant impact on the reaction speed. Therefore, the effect of pH was investigated by CV in 0.1 M PBS over the range from pH 3.0 to 8.0. Plots of peak current against pH are shown in Fig. S2A. It is apparent that the highest peak currents were obtained at pH 5.0, when pH > 5.0 the anodic and cathodic peak currents decreased with increasing pH. Therefore, pH 5.0 was chosen for the subsequent analytical experiments. Fig. S2B shows the anodic and cathodic peak potentials shifted linearly to negative direction with the increasing pH values from 3.0 to 8.0, suggesting the involvement of proton in the electrode reactions. The relationship between the anodic and cathodic peak potentials and the solution pH could be fit to the equation of E_{pa} (V) = −0.06694 pH + 0.5434 (R = 0.9924) and E_{pc} (V) = −0.06551 pH + 0.4565 (R = 0.9980), respectively. The pH effect on E_{pa} and E_{pc} demonstrated that the number of electrons and protons involved in the DA oxidation process was equal. Therefore, the probable reactions of DA on PTCA-GS/MCNT/IL/GCE were described as Scheme 1.

3.4.3. Effect of potential scan rate

Fig. S3 shows the CV of PTCA-GS/MCNT/IL/GCE in 0.1 M PBS (pH 5.0) containing 100 μM DA with scan rate ranging from 30 to 500 mV s^{-1}. The relation between redox peak currents and the scan rate predicted a hybrid kinetic process. At lower scan rates

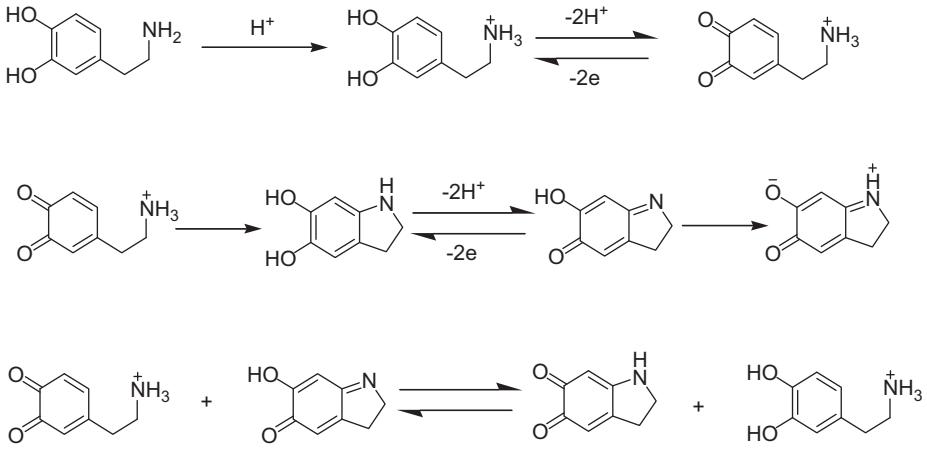

Scheme 1. Possible reaction process of DA on the electrode

(from 30 to 200 mV s^{-1}), both the oxidation and reduction peak currents were linearly proportional to the square root of scan rate. The regression equations was i_{pa} (μA) = −4.9364 v (mV$^{1/2}$ $s^{-1/2}$) − 0.9606 and i_{pc} (μA) = 2.8014 v (mV$^{1/2}$ $s^{-1/2}$) + 1.0137, with a correlation coefficient of 0.9961 and 0.9915, respectively. It suggested that the electrochemical redox behavior of DA at the PTCA-GS/MCNT/IL/GCE surface was a diffusion-controlled process. Whereas at higher scan rates (from 230 to 500 mV s^{-1}), the redox peak currents increased linearly with the increase of scan rate and the regression equations were i_{pa} (μA) = −0.0111 v (mV s^{-1}) − 12.4036 and i_{pc}(μA) = 0.0155 v (mV s^{-1}) + 10.5496, with a correlation coefficient of 0.9907 and 0.9954, respectively. It indicated that the electrochemical oxidation of DA was typical adsorption controlled process. These phenomena suggested that, at low scan rates, DA can easily permeate through PTCA-GS/MCNT/IL film to reach the surface of the electrode by diffusion only. However, at high scan rates, there was not enough time for diffusion of DA through the PTCA-GS/MCNT/IL film, and the electrochemical oxidation process was an absorption behavior. It could be concluded that the reaction occurs not only at the outer surface of electrode but also at reactive sites within the adsorbed assembly.

3.5. Selective determination of DA in the presence of AA and UA

The differential pulse voltammetry (DPV) was used for the determination of DA in the presence of 500 μM AA and 330 μM UA under the optimum conditions. The voltammograms of solutions with different concentrations of DA are shown in Fig. 4. The peak currents were proportional to DA concentration in the range of 0.03 μM–3.82 mM with a detection limit of 1.2×10^{-9} M (S/N = 3).

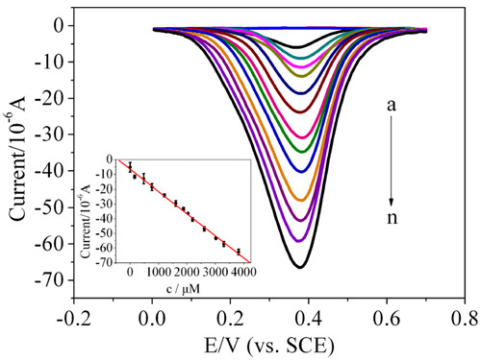

Fig. 4. DPVs for various concentrations of DA in the presence of 500 μM AA in the range of 0.03 μM–3.82 mM (from a to n) in 0.1 M PBS. Inset: Corresponding linear calibration curve of peak current vs. DA concentration. Pulse amplitude: 50 mV, pulse width: 50 ms, pulse period: 0.2 s.

The linear relationship was described as: I (μA) = −6.5501 − 0.0150 c (μM) (R = 0.9982, RSD = 1.15, N = 13)

A comparison of the PTCA-GS/MCNT/IL modified electrode with other reported modified electrodes for DA detection in the presence of AA is listed in Table 1. It can be seen that the proposed method was fairly sensitive and has a large linear range and low detection limit.

3.6. Stability and reproducibility of the modified electrode

The stability of the modified electrode was evaluated. After two-week storage at 4 °C, 97.5% of the initial current signal was obtained and after four-week storage, 95.2% signal remained, indicating that the prepared electrode had excellent long-term stability. Meanwhile, the reproducibility of this modified electrode was investigated and the relative standard deviation (RSD) of the sensor response to 0.78 mM DA was 2.69% for fifteen successive measurements. When five modified electrodes from the same fabrication procedure were prepared and used for the determination of DA solution, and the RSD was 3.9%. These results indicated that the biosensor had good detecting and fabrication reproducibility, and excellent long-term stability.

3.7. Analytical applications

In order to evaluate the validity of the proposed method, the modified electrode was applied to determine DA in Dopamine Hydrochloride Injection (10 mg mL^{-1}). The sample was diluted 10-times with double distilled water and then appropriate amounts of the sample were transferred to an electrolytic cell for the determination using DPV. The analytical results are shown in Table S1. It can be seen that DA in the sample could be satisfactorily detected with a recovery of 97.8%–103.5%, and the RSD (n = 5) was less than 3.0%.

4. Conclusions

A novel and simple strategy for the sensitive detection of DA at PTCA-GS/MCNT/IL modified electrode was presented in this paper. The experimental results demonstrated that the PTCA-GS/MCNT/IL modified electrode exhibited excellent electrocatalytic activity towards the oxidation of DA with good sensitivity, wide linear range and low detection limit. Meanwhile, the proposed method was successfully applied to the determination of DA in Dopamine Hydrochloride Injection with satisfactory results. Functionalized graphene may offer a promising platform for developing highly sensitive and stable electrochemical biosensors.

Table 1
Comparison of different modified electrodes for DA determination.

Electrodes	pH	Linear range (M)	Detection Limit (M)	Reference
Boron-doped CNT/GCE*	7	2.0×10^{-8}–7.5×10^{-5}	1.4×10^{-9}	Deng et al. (2009)
MCNT-IL-Gel/GCE	7	1.0×10^{-6}–1.0×10^{-4}	1.0×10^{-7}	Zhao et al. (2005)
GS/DMF/GCE	7.4	4.0×10^{-6}–1.0×10^{-4}	2.64×10^{-6}	Kim et al. (2010)
GS/CS/GCE	7	5.0×10^{-6}–2.0×10^{-4}	–	Wang et al. (2009)
MCNT-poly(DBA)/GCE	7.4	1.0×10^{-7}–7.0×10^{-5}	1.0×10^{-8}	Zhou et al. (2010)
EDTA-GS/Nafion/GCE	7.2	2.0×10^{-7}–2.5×10^{-5}	1.0×10^{-8}	Hou et al. (2010)
PTCA-GS/MCNT/IL/GCE	5	3.0×10^{-8}–3.8×10^{-3}	1.2×10^{-9}	Present work

* GCE: glassy carbon electrode; CNTs: carbon nanotubes; MCNTs: multi-wall carbon nanotubes; IL: ion liquids; GS: graphene sheets; DMP: dimethyl formamide; CS: chitosan; poly(DBA): poly(3,5-dihydroxy benzoic acid); PTCA-GS: 3,4,9,10-perylene tetracarboxylic acid functionalized graphene sheets.

Acknowledgments

This work was supported in part by the National Natural Science Foundation (20873101), the Project of International Cooperation between China and Ukraine (043-05), and Key Lab of Eco-environment Related Polymer Material of MOE, China.

Appendix A. Supporting information

Supplementary data associated with this article can be found in the online version at http://dx.doi.org/10.1016/j.bios.2012.08.025.

References

Ali, S.R., Ma, Y.F., Parajuli, R.R., Balogun, Y., Lai, W.Y.C., He, H.X., 2007. Analytical Chemistry 79, 2583–2587.
Balamurugan, A., Chen, S.M., 2007. Analytica Chimica Acta 596, 92–98.
Cao, L., Wang, X., Meziani, M.J., Lu, F., Wang, H., Luo, P.G., Lin, Y., Harruff, B.A., Veca, L.M., Murray, D., Xie, S.Y., Sun, Y.P., 2007. Journal of the American Chemical Society 129, 11318–11319.
Chen, Y., Liu, H., Ye, T., Kim, J., Mao, C., 2007. Journal of the American Chemical Society 129, 8696–8697.
Choi, B.G., Park, H.S., Park, T.J., Kim, D.H., Lee, S.Y., Hong, W.H., 2009. Electrochemistry Communications 11, 672–675.
Codognoto, L., Winter, E., Paschoal, J.A.R., Suffredini, H.B., Carbral, M.F., Machado, S.A.S., Rath, S., 2007. Talanta 72, 427–433.
Dai, X., Wildgoose, G.G., Salter, C., Crossley, A., Compton, R.G., 2006. Analytical Chemistry 78, 6102–6108.
Deng, C.Y., Chen, J.H., Wang, M.D., Xiao, C.H., Nie, Z., Yao, S.Z., 2009. Biosensors and Bioelectronics 24, 2091–2094.
Fang, B., Zhang, C.H., Zhang, W., Wang., G.F., 2009. Electrochimica Acta 55, 178–182.
Fu, C.C., Lee, H.Y., Chen, K., Lim, T.S., Wu, H.Y., Lin, P.K., Wei, P.K., Tsao, P.H., Chang, H.C., Fann, W., 2007. Proceedings of the National Academy of Sciences of the United States of America 104, 727–732.
Guldi, D.M., Rahman, G.M.A., Zerbetto, F., Ptato, M., 2005. Accounts of Chemical Research 38, 871–878.
Geim, A.K., Novoselov, K.S., 2007. Nature Materials 6, 183–191.
Hao, C., Ding, L., Zhang, X., Ju, H., 2007. Analytical Chemistry 79, 4442–4447.
Hong, W.J., Bai, H., Xu, Y.X., Yao, Z.Y., Gu, Z.Z., shi, G.Q., 2010. Journal of Physical Chemistry C 114, 1822–1826.
Hou, S.F., Kasner, M.L., Su, S.J., Patel, K., Cuellari, R., 2010. Journal of Physical Chemistry C 114, 14915–14921.
Kalimuthu, P., Abraham, J.S., 2010. Talanta 80, 1686–1691.
Kim, Y.R., Bong, S.Y., Kang, Y.J., Yang, Y., Mahajan, R.K., Kim, J.S., Kim, H., 2010. Biosensors and Bioelectronics 25, 2366–2369.
Lakshmi, D., Bossi, A., Whitcombe, M.J., Chianella, I., Fowler, S.A., Subrahmanyam, S., Piletska, E.V., Piletsky, S.A., 2009. Analytical Chemistry 81, 3576–3584.
Li, D., Muller, M.B., Gilje, D., Kaner, R.B., Wallace, G.G., 2008. Nature Nanotechnology 3, 101–105.
Li, F.H., Yang, H.F., Shan, C.S., Zhang, Q.X., Han, D.X., Ivaskab, A., Niu, L., 2009. Journal of Materials Chemistry 19, 4022–4025.
Liu, A.H., Honma, I., Zhou, H.S., 2005. Biosensors and Bioelectronics 21, 809–816.
Liu, K.P., Zhang, J.J., Yang, G.H., Wang, C.M., Zhu, J.J., 2010. Electrochemistry Communications 12, 402–405.
Liu, Y., Huang, J.S., Hou, H.Q., You, T.Y., 2008b. Electrochemistry Communications 10, 1431–1434.
Liu, Z., Li, X., Tabakman, S.M., Jiang, K., Fan, S., Dai, H., 2008a. Journal of the American Chemical Society 130, 13540–13541.
Mo, J.W., Ogorevc, B., 2001. Analytical Chemistry 73, 1196–1202.
Pandey, S., 2006. Analytica Chimica Acta 556, 38–45.
Rodney, A., David, J., Dali, Q., Terry, R., 2002. Accounts of Chemical Research 35, 1008–1110.
Rodriguez, M.C., Rubianes, M.D., Rivas, G.A., 2008. Journal of Nanoscience and Nanotechnology 8, 6003–6009.
Shul, G., Plenet, J.S., Gaillon, L., Opallo, M., 2006. Electrochemistry Communications 8, 1111–1114.
Sun, W., Gao, R.F., Jiao, K., 2007. Chinese Journal of Analytical Chemistry 35, 1813–1819.
Sun, W., Jiang, Q., Wang, Y., Jiao, K., 2009a. Sensors and Actuators B 136, 419–424.
Sun, W., Li, X.Q., Wang, Y., Zhao, R.J., Jiao, K., 2009b. Electrochimica Acta 54, 4141–4148.
Tang, C.F., Kumar, S.A., Chen, S.M., 2008. Analytical Biochemistry 380, 174–183.
Thiagarajan, S., Tsai, T.H., Chen, S.M., 2009. Biosensors and Bioelectronics 24, 2712–2715.
Wang, Y., Li, Y.M., Tang, L.H., Lu, J., Li, J.H., 2009. Electrochemistry Communications 11, 889–892.
Yen, G.C., Duh, P.D., Tsai, H.L., 2002. Food Chemistry 79, 307–313.
Zhang, Q., Wu, S.Y., Zhang, L., Lu, J., 2011. Biosensors and Bioelectronics 26, 2632–2637.
Zhao, Y.F., Gao, Y.Q., Zhan, D.P., Liu, H., Zhao, Q., Kou, Y., Shao, Y.H., Li, M.X., Zhuang, Q.K., Zhu, Z.W., 2005. Talanta 66, 51–57.
Zhou, X., Zheng, N., Hou, S.R., Li, X.J., Yuan, Z.B., 2010. Journal of Electroanalytical Chemistry 642, 30–34.
Zhu, S.Y., Li, H.J., Niu, W.X., Xu, G.B., 2009. Biosensors and Bioelectronics 25, 940–943.